A Spectroscopic and Theoretical Study of the Reactions of Group 6 Metal Atoms with Carbon Dioxide

Philip F. Souter and Lester Andrews*

Contribution from the Department of Chemistry, University of Virginia, Charlottesville, Virginia 22901

Received April 1, 1997[⊗]

Abstract: Group 6 metal atoms, generated by laser ablation, react with CO_2 to give the insertion products OMCO and $O_2M(CO)_2$ (M = Cr, Mo, or W) which have been isolated in argon matrices and identified by the effects of isotopic substitution on their infrared spectra. These assignments have been supported by DFT calculations, and the theoretical and experimental spectra are in excellent agreement. Other products include the molecules O_2MCO, MO, and MCO and the CO_2 complex Cr (η^1-**O**CO) which, upon irradiation with UV-light, will photoisomerize to give OCrCO, an interesting example of photoactivation of CO_2.

Introduction

Carbon dioxide is a naturally abundant carbon source that has been implicated as a contributor to the predicted global warming often referred to as the "greenhouse effect". The most important CO_2 activation process is photosynthesis, but little is known about the mode of ligation of the CO_2 to the metal ion present in the active enzyme. The interaction between CO_2 and transition metal centers is receiving increased attention[1−4] as the possibilities of recycling CO_2 generated in industrial emissions[5] and also of replacing petroleum with carbon dioxide as the starting material for the synthesis of fine chemicals[6] both represent exciting and important goals. Previous studies of the interaction of metal atoms with CO_2 in low-temperature matrices focused on the interaction of Li,[7] Cs,[8] and Al[9] with CO_2. Additionally the interaction of several of the thermally generated first-row transition metal atoms, including Cr, with CO_2 has been investigated both experimentally in solid CO_2[10] and theoretically.[11] In this laboratory, the reactions of laser-ablated B, U, Ti, and Be atoms with CO_2 have been investigated, and all four were found to insert into CO_2 to give OMCO (M = B, U, Ti, or Be) as the primary reaction product.[12−15] Much attention has been devoted to the organometallic chemistry of CO_2 and a comprehensive review has recently been published.[4] The main problem with the chemistry of CO_2, lies in its inherent

thermodynamic stability, and methods of "activating" CO_2 are consequently actively being sought.

We have studied the reactions between laser-ablated group 6 metal atoms and CO_2/Ar mixtures and have trapped the reaction products, including OMCO and $O_2M(CO)_2$, in argon matrices and identified them by the effects of isotopic substitution upon their infrared spectra. These assignments have been confirmed by comparison between the experimentally observed frequencies, relative intensities, and isotope ratios and those predicted by DFT-based calculations. A preliminary communication on this work has appeared.[16]

Experimental Section

The technique used for matrix investigation of the reactions of pulsed laser-ablated metal atoms has been detailed previously.[12−15,17,18] FTIR spectra were recorded on a Nicolet 550 at 0.5 cm^{-1} resolution. Typically mixtures of between 0.5% and 2% carbon dioxide in argon were deposited at a rate of *ca.* 3 mmol/h for 1−2 h onto a CsI window held at 6−7 K while the metals were ablated using 30−50 mJ pulses of YAG 1064 nm fundamental. After deposition the samples were annealed to 20 K, photolyzed using a 175 W mercury street lamp (Philips H39KB) with the globe removed (240−580 nm range), and then further annealed, typically to 30 and 35 K.

C^{18}O$_2$ was synthesized either by heating graphite with ^{18}O$_2$ (Yeda) in a quartz tube or, more efficiently, by discharging a 2:1 mixture of C^{18}O and ^{18}O$_2$ in a 3 L glass bulb with an attached finger held at 77 K to trap the C^{18}O$_2$ thus formed. The latter reaction proved to be essentially quantitative after 15 min and was also used to synthesize a 1:2:1 mixture of C^{16}O$_2$/C^{16}O^{18}O/C^{18}O$_2$ from a 2:1 mixture of C^{18}O and ^{16}O$_2$. The isotopic carbon dioxide samples thus produced were freed from any residual traces of oxygen, ozone, or carbon monoxide by pumping on the sample at *ca.* 135 K. Samples of CO_2 (Matheson) and $^{13}CO_2$ (Cambridge Isotopes) were used without further purification (the $^{13}CO_2$ sample contained *ca.* 10% ^{18}O).

Theoretical Section

DFT calculations were performed using both the Amsterdam Density Functional Code (ADF 2.0.1)[19] and Gaussian 94[20] suite of programs. The ADF calculations employed the Vosko−Wilk−Nusair potential in the context of the local density approximation (LDA), along with the Becke (B) and Perdew

[⊗] Abstract published in *Advance ACS Abstracts,* July 15, 1997.

(1) Ibers, J. A. *Chem. Soc. Rev.* **1982,** *11*, 57.

(2) Creutz, C. In *Electrochemical and Electrocatalytic Reactions of Carbon Dioxide*; eds. Sullivan, B. P., Krist, K., Guard, H. E., Eds.; Elsevier: Amsterdam, 1993; Chapter 2.

(3) Arreseta, M.; Quarntana, E.; Tommasi, I. *New J. Chem.* **1994,** *18*, 133.

(4) Gibson, D. H. *Chem. Rev.* **1996,** *96*, 2063.

(5) Halmann, M. M. *Chemical Fixation of Carbon Dioxide. Methods for Recycling CO₂ into Useful Products*; CRC Press: Boca Raton, FL, 1993.

(6) See for example, Cutler, A. R.; Hanna, P. K.; Vites, J. C. *Chem. Rev.* **1988,** *88*, 1363.

(7) Kafafi, Z. H.; Hauge, R. H.; Billups, W. E.; Margrave, J. L. *J. Am. Chem. Soc.* **1983,** *105*, 3886.

(8) Kafafi, Z. H.; Hauge, R. H.; Billups, W. E.; Margrave, J. L. *Inorg. Chem.* **1984,** *23*, 177.

(9) LeQuere, A. M.; Xu, C.; Manceron, L. *J. Phys. Chem.* **1991,** *95*, 3031.

(10) Mascetti, J.; Tranquille, M. *J. Phys. Chem.* **1988,** *92*, 2177.

(11) Yeung, G. H. *Mol. Phys.* **1988,** *65*, 669.

(12) Burkholder, T. R.; Andrews, L. *J. Phys. Chem.* **1993,** *97*, 3500.

(13) Tague, T. J., Jr.; Andrews, L.; Hunt, R. D. *J. Phys. Chem.* **1993,** *97*, 10920.

(14) Chertihin, G. V.; Andrews, L. *J. Am. Chem. Soc.* **1995,** *117*, 1595.

(15) Andrews, L.; Tague, T. J., Jr. *J. Am. Chem. Soc.* **1994,** *116*, 6856.

(16) Souter, P. F.; Andrews, L. *Chem. Commun.* **1997,** 777.

(17) Burkholder, T. R.; Andrews, L. *J. Chem. Phys.* **1991,** *95*, 8697.

(18) Souter, P. F.; Kushto, G. P.; Andrews, L.; Neurock, M. *J. Am. Chem. Soc.* **1997,** *119*, 1682.

(19) ADF 2.0.1, Theoretical Chemistry, Vrije Universiteit, Amsterdam.

(P) gradient corrections to the exchange and correlation energies. Nonlocal gradient corrections were explicitly accounted for in each SCF cycle. ADF employs a series of Slater basis functions, and the adjustable parameter controlling the accuracy of the numerical integration[21] was set at a value of either 5.0 or usually 6.0. A triple ζ basis set was used for the metals, and a triple ζ basis set with polarization was used for carbon and oxygen. Additionally for both molybdenum and tungsten the core electrons were frozen up to the 3d and 5p levels, respectively, to treat relativistic core effects. Quasirelativistic corrections were employed using the Pauli formalism with corrected core potentials. The quasirelativistic frozen core shells were generated using the auxiliary program DIRAC.[19] The resultant approach has been shown to improve results considerably over first-order treatments.[22,23]

Geometry optimizations and frequency calculations were also run using the Gaussian 94 suite of programs. These too utilized a DFT-based approach with the Becke 1988 exchange functional (B) and Perdew correlational functional (P86). For oxygen and carbon the Dunning/Huzinaga full double ζ basis sets were used with one added polarization function (D95*). For chromium, molybdenum, and tungsten the Los Alamos ECP plus DZ basis sets were chosen (LanL2DZ). Optimized energies, geometries (all quoted bond lenths in angstroms and angles in degrees), frequencies, and the effects of isotopic substitution upon these frequencies were calculated, and the values of $\langle S^2 \rangle$ indicate minimal artificial spin contamination in these calculations.

Results and Discussion

Figures 1−3 show the infrared spectra of the products generated by the reaction of laser-ablated Cr, Mo, and W atoms, respectively, with 2% CO_2 in Ar mixtures isolated at 6−7 K, together with the effects of annealing and broad band UV-photolysis on these deposits. Figures 4−6 show the effects of isotopic substitution upon the infrared spectra of such matrix-isolated deposits arising from the reactions of Cr, Mo, and W, respectively, with CO_2 in Ar. The frequencies of the observed bands from the reactions of CO_2 and its various isotopomers with Cr, Mo and W, together with their proposed assignments are presented in Tables 1−3.

In the ensuing section, for each molecule the experimentally observed frequencies (cm^{-1}) are quoted in parentheses and those separated by a semicolon refer to the values observed for chromium, molybdenum, and tungsten, respectively. For both chromium and molybdenum some of the observed bands showed fully resolvable isotopic splittings due to the natural abundances of the metal isotopes, and the quoted numbers in the text refer to the values observed for ^{52}Cr and ^{98}Mo. In all experiments CO or its appropriate isotopic forms were observed as well as the CO_2 complex of CO, which appears as a shoulder at slightly higher frequency.[15]

OMCO. The dominant product from the reactions of group 6 metal atoms with 0.5% CO_2/Ar mixtures is the direct insertion

(20) Gaussian 94: Frisch, M. J.; Trucks, G. W.; Schlegel, H. B.; Gill, P. M. W.; Johnson, B. G.; Robb, M. A.; Cheeseman, J. R.; Keith, T. A.; Petersson, G. A.; Montgomery, J. A.; Raghavachari, K.; Al-Laham, M. A.; Zakrzewski, V. G.; Ortiz, J. V.; Foresman, J. B.; Cioslowski, J.; Stefanov, B. B.; Nanayakkara, A.; Challacombe, M.; Peng, C. Y.; Ayala, P. Y.; Chen, W.; Wong, M. W.; Andres, J. L.; Replogle, E. S.; Gomperts, R.; Martin, R. L.; Fox, D. J.; Binkley, J. S.; Defrees, D. J.; Baker, J.; Stewart, J. P.; Head-Gordon, M.; Gonzalez, C.; Pople, J. A., Gaussian Inc., Pittsburgh, PA, 1995.
(21) teVelde, B.; Baerends, E. J. *J. Comput. Phys.* **1992**, *99*, 84 and references cited therein.
(22) Ziegler, T. Calculations of bond energies in heavy element compounds. Ph.D. Thesis, Vrije Universiteit, Amsterdam, 1987. Heinemann, C.; Cornehl, H. H; Schroder, D.; Dolg, M.; Schwarz, S. *Inorg. Chem.* **1996**, *35*, 2463.
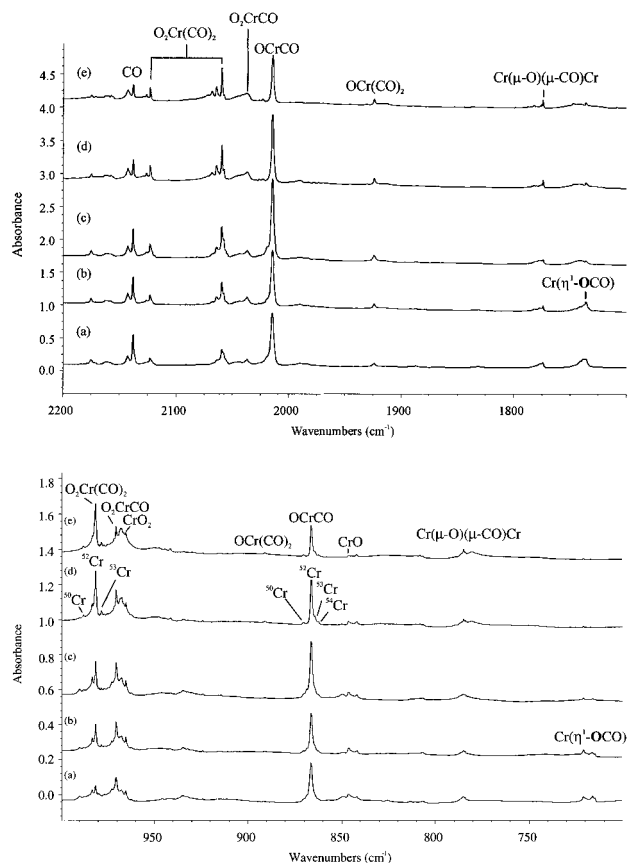(23) Ziegler, T. *Chem. Rev.* **1991**, *91*, 651.

Figure 1. Infrared spectra of the matrix-isolated products from the reaction of laser-ablated Cr with 2% CO_2 in argon after (a) 1 h of deposition, (b) annealing to 20 K, (c) broad band UV-photolysis, (d) annealing to 30 K, and (e) annealing to 35 K.

product OMCO. Full details are given in Tables 1−3 for all three metals which behave in an analogous fashion. The two most intense bands for the OMCO molecule are the CO (2014.4, 1847.0, 1879.0) and MO (866.3, 951.8, 969.6) stretching fundamentals. Experiments run with $^{13}CO_2$ (1969.7, 866.3; 1804.3, 952.4; 1837.0, 969.6) and $C^{18}O_2$ (1967.3, 829.5; 1806.1, 905.3; 1838.8, 918.9), respectively, confirm that each molecule contains a CO and a MO group, on the basis of comparison of observed isotopic frequency ratios with calculated harmonic diatomic ratios. Experiments run with $^{12}CO_2/^{13}CO_2$, $C^{16}O_2/C^{18}O_2$, and $C^{16}O_2/C^{16}O^{18}O/C^{18}O_2$ all revealed isotopic doublets in the CO stretching region, and the latter two revealed doublets in the MO stretching region. This isotopic pattern confirms the presence of *exactly* one CO group and *exactly* one MO group, allowing definitive spectral assignment of these bands to the OMCO molecules. For both chromium and molybdenum, isotopic splittings due to the natural abundances of the metal isotopes were observed for the MO stretching fundamental, and the observed statistical distribution confirmed the presence of *exactly* one metal atom. In experiments run with Cr and Mo with $^{13}CO_2$, the ^{18}O impurity in the sample proved sufficiently large to observe the CO stretch of $OM^{13}C^{18}O$, which occurred at 1921.4 and 1762.4 cm^{-1} for Cr and Mo, respectively.

In the experiments with chromium and CO_2, a higher energy combination band was observed at 2175.4 cm^{-1}. This band shifted to 2126.7 cm^{-1} on reaction with $^{13}CO_2$ and 2124.9 cm^{-1} on reaction with $C^{18}O_2$ and, as well as shadowing the bands due to the CO and CrO stretches of this molecule upon annealing and photolysis, also appears as a doublet in experiments run with $^{12}CO_2/^{13}CO_2$, $C^{16}O_2/C^{16}O^{18}O/C^{18}O_2$, and $C^{16}O_2/C^{18}O_2$. For tungsten it proved possible to locate one of the low-energy heavily mixed modes, consisting of partly W−C stretch and
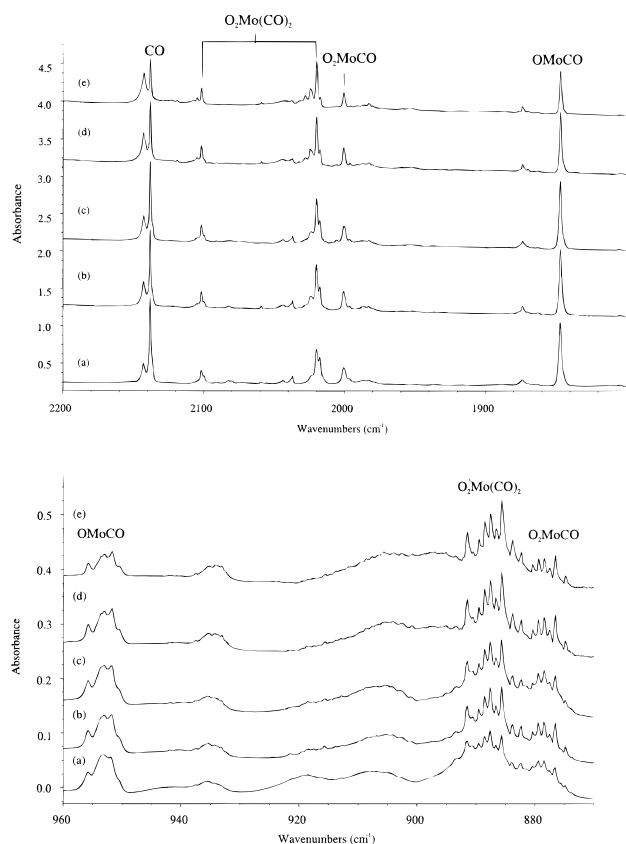
Figure 2. Infrared spectra of the matrix-isolated products from the reaction of laser-ablated Mo with 2% CO_2 in argon after (a) 1 h of deposition, (b) annealing to 20 K, (c) broad band UV-photolysis, (d) annealing to 30 K, and (e) annealing to 35 K.

partly CO bend. The feature occurs at 483.8 cm^{-1} in the ^{12}-CO_2 spectrum, 469.1 cm^{-1} in the $C^{18}O_2$ spectrum, and 477.6 cm^{-1} in the $^{13}CO_2$ spectrum. It appears as a doublet in experiments run with $^{12}CO_2/^{13}CO_2$, $C^{16}O_2/C^{16}O^{18}O/C^{18}O_2$, and $C^{16}O_2/C^{18}O_2$ and displays exactly the same annealing and photolysis behavior as the CO and WO stretching modes associated with this molecule. The observed isotope shifts (6.2 cm^{-1} from OWCO to OW^{13}CO and 14.7 cm^{-1} from OWCO to OWC^{18}O) find very pleasing agreement with those calculated (6.9 cm^{-1} from OWCO to OW^{13}CO and 14.3 cm^{-1} from OWCO to OWC^{18}O) using the Gaussian 94 program, as detailed in Table 4.

The effects of annealing and photolysis on the samples are shown in Figures 1−3. As can be seen the features due to the OCrCO molecule grow upon annealing to 20 K and upon photolysis but decrease upon annealing to 30 and 35 K. OMoCO displayed similar annealing properties although the photolytic growth was not quite as marked. The bands due to OWCO increased upon initial annealing to 20 K, decreased upon photolysis, increased upon annealing to 30 K, and decreased upon annealing to 35 K.

Optimized energies, frequencies, and, in the case of the calculations using Gaussian 94, isotope shifts are presented in Table 4. Calculations using either the Gaussian 94 program or ADF 2.0.1 predict the vibrational frequencies of these molecules to within a few percent of the values observed in an argon matrix. The calculated and observed relative intensities of the vibrations also match remarkably well. For all three OMCO molecules the agreement between the observed and calculated isotopic ratios, $\nu_{12/13}$ and $\nu_{16/18}$, is excellent, confirming both the identification of the molecules and the accuracy of the calculations used to predict their mechanics of vibration.
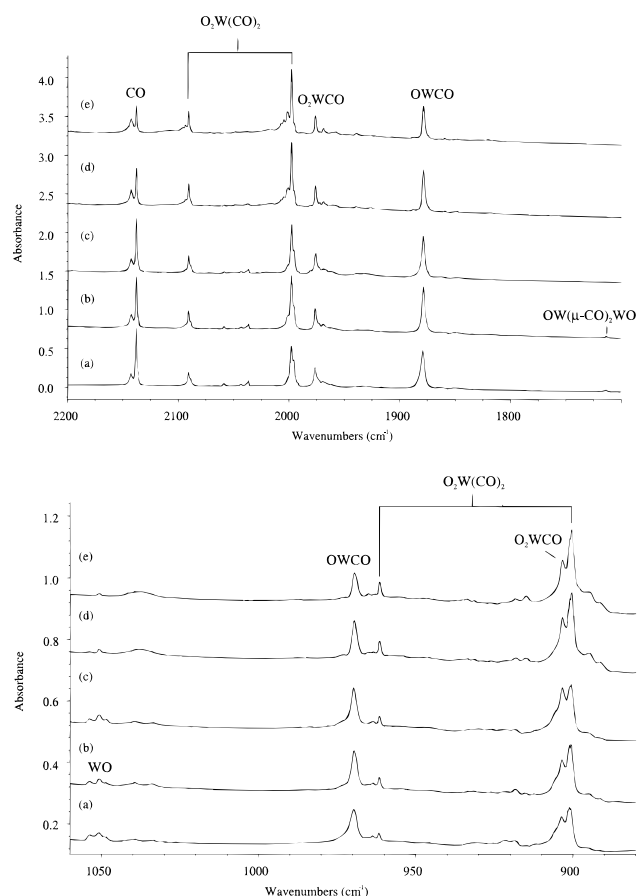

Figure 3. Infrared spectra of the matrix-isolated products from the reaction of laser-ablated W with 2% CO_2 in argon after (a) 1 h of deposition, (b) annealing to 20 K, (c) broad band UV-photolysis, (d) annealing to 30 K, and (e) annealing to 35 K.

The observation of direct insertion of laser-ablated chromium atoms into CO_2 is in contrast to an earlier study of thermal chromium atoms in a pure CO_2 matrix where there was no evidence for insertion.[10,24]

$O_2M(CO)_2$. The other main product from these reactions proved to arise from the insertion of the metal atoms into two CO_2 molecules. As might be anticipated by raising the concentration of CO_2 from 0.5% to 2%, the relative yield of $O_2M(CO)_2$ to OMCO increases. For all three molecules two bands were observed in the CO stretching region (2123.2, 2059.7; 2101.9, 2020.1; 2091.1, 1998.2) corresponding to the symmetric and antisymmetric CO stretches of the $O_2M(CO)_2$ molecules, while in the MO stretching region the antisymmetric MO_2 stretches were seen for all three molecules (981.4, 885.6, 901.1), but the much weaker symmetric stretches were only seen for chromium (941.6) and tungsten (961.6). Reaction with ^{13}-CO_2 confirmed that the two highest bands (2074.8, 2013.8; 2053.9, 1975.4; 2042.9, 1953.6) are indeed due to CO stretches, while the bands in the oxide region showed no apparent shift, confirming that carbon was not involved in these modes. Reaction with $C^{18}O_2$ confirmed further that the higher two bands (2075.3, 2011.6; 2054.7, 1972.7; 2045.1, 1953.6) were due to CO stretches and that the antisymmetric MO_2 stretching modes (945.1; 846.1; 856.1) and symmetric stretching CrO_2 (892.2)

(24) The band observed in ref 10 at 960 cm^{-1}, tentatively assigned to a CO_2 reaction product, occurs at very nearly the same energy as the antisymmetric stretch of CrO_2 (Chertihin, G. V.; Bare, W. D.; Andrews, L. *J. Chem. Phys.*, in press), an almost inevitable impurity in a reaction involving thermally generated chromium atoms. With no isotopic data and no associated carbonyl stretches, this band is most likely due to CrO_2 in a CO_2 matrix.
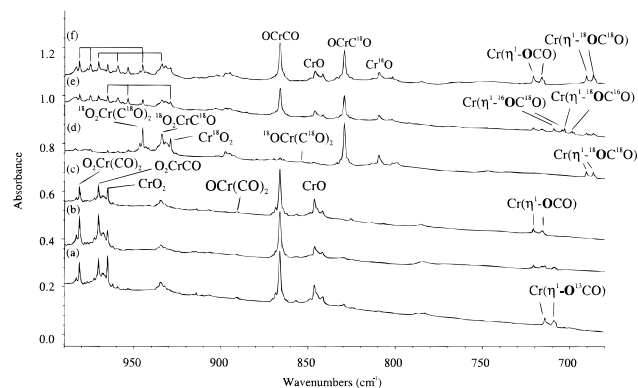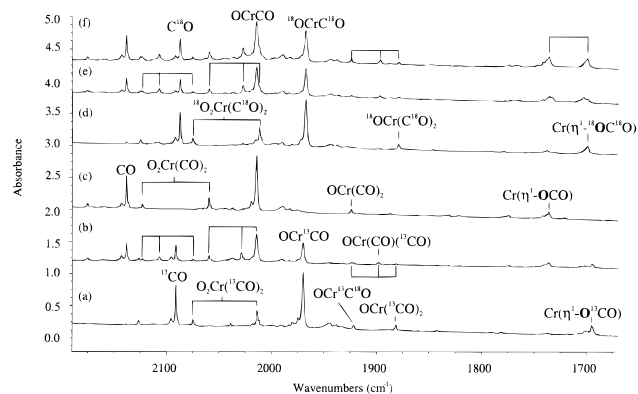
Figure 4. Infrared spectra of the reaction products of Cr and 0.5% CO_2 after annealing to 20 K: (a) $^{13}CO_2$; (b) $CO_2/^{13}CO_2$; (c) CO_2; (d) $C^{18}O_2$; (e) $CO_2/C^{16}O^{18}O/C^{18}O_2$; (f) $CO_2/C^{18}O_2$.
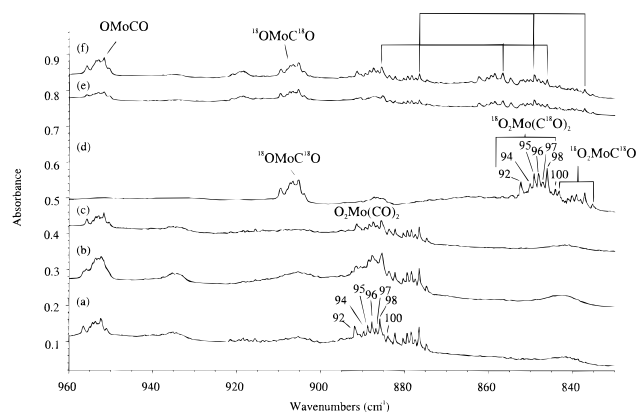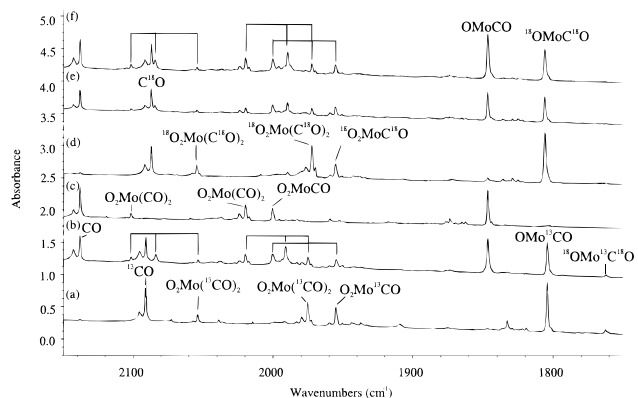
Figure 5. Infrared spectra of the reaction products of Mo and 0.5% CO_2 after annealing to 30 K: (a) $^{13}CO_2$; (b) $CO_2/^{13}CO_2$; (c) CO_2; (d) $C^{18}O_2$; (e) $CO_2/C^{16}O^{18}O/C^{18}O_2$; (f) $CO_2/C^{18}O_2$.

and WO_2 (909.4) modes were indeed metal oxide stretches. Reaction with either $C^{16}O_2/C^{18}O_2$ or $C^{16}O_2/C^{16}O^{18}O/C^{18}O_2$ gave
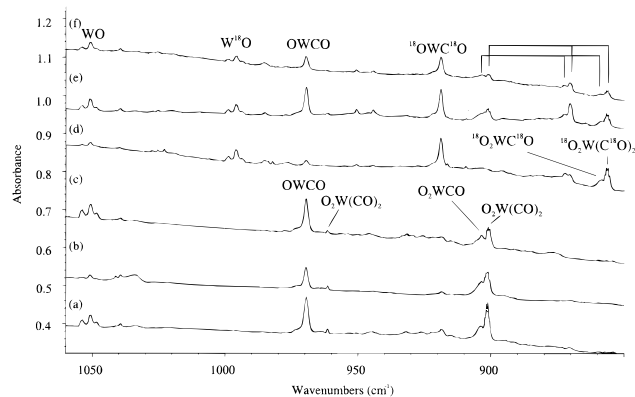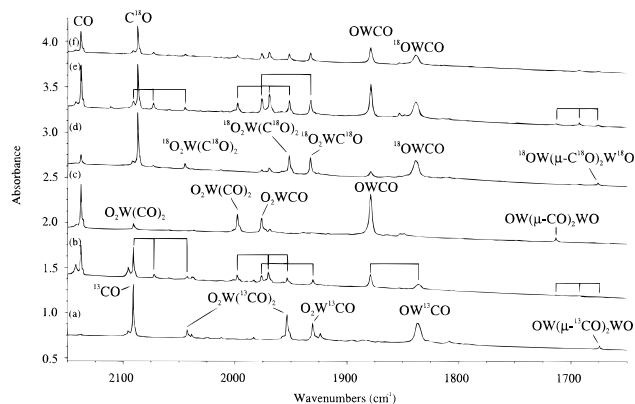
Figure 6. Infrared spectra of the reaction products of W and 0.5% CO_2 after annealing to 20 K: (a) $^{13}CO_2$; (b) $CO_2/^{13}CO_2$; (c) CO_2; (d) $C^{18}O_2$; (e) $CO_2/C^{16}O^{18}O/C^{18}O_2$; (f) $CO_2/C^{18}O_2$.

rise to 1:2:1 asymmetric triplets for all these bands, details of which can be found in Tables 1−3. This is indicative of the presence of *precisely* two equivalent CO groups and *precisely* two equivalent oxygen atoms and confirms that the two oxygens and CO groups bound to the metals must come from two different CO_2 molecules. Reaction with a $^{12}CO_2/^{13}CO_2$ mixture revealed a 1:2:1 isotopic triplet for both CO stretching fundamentals, further confirming the presence of two equivalent CO groups. In the cases of chromium and molybdenum, the presence of *exactly* one metal atom is clearly demonstrated by the statistical distribution of the metal isotopic pattern for the M−O antisymmetric stretching fundamental, as illustrated in Figures 1 and 5. For all three molecules the agreement between the experimental and theoretical spectra, details of which can be found in Table 5, is extremely good.

For all three metals it proved possible to observe one of the lower energy modes, which involved primarily the metal−carbon antisymmetric stretching motion. The spectra of the matrix-isolated products from the reaction of molybdenum with CO_2 showed a weak band at 541.3 cm^{-1} which displays the same annealing and photolysis behavior as the rest of the bands associated with the molecule as well as preserving a constant relative intensity to the other bands in all experiments. The band shifts 4.8 cm^{-1}(*cf.* 4.8 cm^{-1} calculated) on reaction with $C^{18}O_2$ and 14.5 cm^{-1} (*cf.* 15.5 cm^{-1} calculated) on reaction with $^{13}CO_2$. Appropriate isotopic triplets at 541.3, 534.6, and 526.7 cm^{-1} (*cf.* 543.3, 535.8, and 527.8 cm^{-1} calculated) are observed in the reactions with $^{12}CO_2/^{13}CO_2$ and at 541.3, 538.8, and 536.5 cm^{-1} (*cf.* 543.3, 541.1, and 538.8 cm^{-1} calculated) in experiments run with $C^{16}O_2/C^{18}O_2$. Calculations predict the presence of several bands in this region for the products arising from the reaction with $C^{16}O_2/C^{16}O^{18}O/C^{18}O_2$, and the weakness of the feature precluded the resolution of these components in the experiment.

Table 1. Observed Infrared Absorptions (cm^{-1}) of the Dominant Products in the Reaction of Laser-Ablated Chromium Atoms with CO_2 Trapped in an Argon Matrix at 6-7 K

molecule	CO_2	$^{13}CO_2$	$^{12}CO_2/^{13}CO_2$	$C^{18}O_2$	$C^{16}O_2/C^{16}O^{18}O/C^{18}O_2$	assignment
OCrCO[a]	2014.4	1969.7	2014.4, 1969.7	1967.3	2014.4, 1967.3	ν(C−O)
	866.3[b]	866.3	866.3	829.5[b]	866.3, 829.5	ν(Cr−O)
	2175.4	2126.7	2175.4, 2126.7	2124.9	2175.4, 2124.9	combination
$O_2Cr(CO)_2$[a]	2123.2	2074.8	2123.2, 2074.8	2075.3	2123.2, 2107.2, 2075.3	ν_s(C−O)[c]
	2059.7	2013.8	2059.7, 2013.8	2011.6	2058.7, 2027.6, 2011.6	ν_{as}(C−O)[c]
	981.4[b]	981.4	981.4	945.1[b]	981.4, 975.4, 945.1	ν_{as}(Cr−O)[c]
	941.6	941.6	941.6	892.2	941.6, 903.0, 892.2	ν_s(Cr−O)[c]
	540.6	527.4	540.6, 534.1, 527.4	534.9	d	ν_{as}(Cr−C)[c]
O_2CrCO[a]	2037.1	1990.0	2037.1, 1990.0	1989.7	2037.1, 1989.7	ν(C−O)
	970.5	970.5	970.5	934.1	970.5, 959.5, 934.1	ν_{as}(Cr−O)[c]
	914.4	914.4	914.4	879.5	924.3, ca. 895.1, 879.5	ν_s(Cr−O)[c]
CrO[a]	846.3	846.3	846.3	809.6	846.3, 809.6	ν(Cr−O)
CrO_2[a]	965.2	965.2	965.2	929.1	965.2, 953.6, 929.1	ν_{as}(Cr−O)[c]
	914.4	914.4	914.4	869.7	914.4, ?, 869.7	ν_s(Cr−O)[c]
$CrCO$	1975.3	1932.4	1975.3, 1932.4	1927.3	1975.3, 1927.3	ν(C−O)
$OCr(CO)_2$[a]	1923.9	1881.2	1923.9, 1897.9, 1881.2	1878.9	1923.9, 1896.5, 1878.9	ν_{as}(C−O)[c]
	891.0	891.0	891.0	853.8	891.0, 853.8	ν(Cr−O)
$Cr(\eta^1$-**O**CO) site 1[a]	1735.6	1694.8	1735.6, 1694.8	1698.9	1735.6, 1732.3, 1702.7, 1698.9	ν_{as}(C−O)[c]
	721.0	714.1	721.0, 714.1	690.5	721.0, 709.3, 703.1, 690.5	ν(Cr−O)
$Cr(\eta^1$-**O**CO) site 2[a]	ca. 1738	ca. 1697	ca. 1738, 1697	ca. 1701	ca. 1738, ?, ?, 1701	ν_{as}(C−O)[c]
	716.1	709.0	716.1, 709.0	686.5	716.1, 704.1, 698.8, 686.5	ν(Cr−O)
$Cr(\mu$-O)(μ-CO)Cr (?)	1773.8	1736.8	1773.8, 1736.8	1737.2	1773.8, 1737.2	ν(C−O)
	785.0	783.4	785.0, 783.4	746.7	785.0, 746.7	ν(Cr−O)

[a] Refers to ^{52}Cr. [b] For OCrCO ($^{18}OCr^{18}O$) the bands due to ^{50}Cr, ^{53}Cr, and ^{54}Cr occurred at 870.4 (833.8), 864.4 (827.5), and 862.6 (825.5), respectively. For $O_2Cr(CO)_2$ ($^{18}O_2Cr(C^{18}O)_2$) the bands due to ^{50}Cr and ^{53}Cr were resolved at 987.9 (951.9) and 978.3 (941.9), respectively. [c] ν_s refers to the symmetric stretching frequency, and ν_{as} refers to the antisymmetric stretching frequency. [d] Owing to the many possible isotopomers and the weakness of this feature, all the intermediate components could not be resolved for this band. A mechanical mixture of $CO_2/C^{18}O_2$ did however yield a 1:2:1 triplet at 540.6, 537.9, and 534.9 cm^{-1}.

Table 2. Observed Infrared Absorptions (cm^{-1}) of the Dominant Products in the Reaction of Laser-Ablated Molybdenum Atoms with CO_2 Trapped in an Argon Matrix at 6-7 K

molecule	CO_2	$^{13}CO_2$	$^{12}CO_2/^{13}CO_2$	$C^{18}O_2$	$C^{16}O_2/C^{16}O^{18}O/C^{18}O_2$	assignment
OMoCO[a]	1847.0	1804.3	1847.0, 1804.3	1806.1	1847.0, 1806.1	ν(C−O)
	951.8	952.4	951.8, 952.4	905.3	951.8, 905.3	ν(Mo−O)
$O_2Mo(CO)_2$[a]	2101.9	2053.9	2101.9, 2084.0, 2053.8	2054.7	2101.9, 2084.6, 2054.7	ν_s(C−O)[b]
	2020.1	1975.4	2020.1, 1991.4, 1975.4	1972.7	2020.1, 1990.0, 1972.7	ν_{as}(C−O)[c]
	885.6	885.6	885.6	846.1	885.6, 856.7, 846.1	ν_{as}(Mo−O)[c]
	541.3	527.8	543.3, 535.8, 527.8	536.5	d	ν_{as}(Mo−C)[c]
O_2MoCO[a]	2000.7	1955.2	2000.7, 1955.2	1955.7	2000.7, 1955.7	ν(C−O)
	876.5	876.5	876.5	837.2	885.6, ca. 849.2, 837.2	ν_{as}(Mo−O)[c]
MoCO	1862.6	1819.2	1862.6, 1819.2	1822.3	1862.6, 1822.3	ν(C−O)

[a] Refers to ^{98}Mo. [b] ν_s refers to the symmetric stretching frequency. [c] ν_{as} refers to the antisymmetric stretching frequency. [d] Not clearly resolved for all the possible isotopomers. For $CO_2/C^{18}O_2$ a triplet is seen at 543.3, 541.1, and 538.8 cm^{-1}.

Table 3. Observed Infrared Absorptions (cm^{-1}) of the Dominant Products in the Reaction of Laser-Ablated Tungsten Atoms with CO_2 Trapped in an Argon Matrix at 6-7K

molecule	CO_2	$^{13}CO_2$	$^{12}CO_2/^{13}CO_2$	$C^{18}O_2$	$C^{16}O_2/C^{16}O^{18}O/C^{18}O_2$	assignment
OWCO	1879.0	1837.0	1879.0, 1837.0	1838.8	1879.0, 1838.8	ν(C−O)
	969.6	969.6	969.6	918.9	969.6, 918.9	ν(W−O)
	483.8	477.6	483.8, 477.6	469.1	483.6. 469.1	ν(W−O)/δ(C−O)
$O_2W(CO)_2$	2091.1	2042.9	2091.1, 2072.7, 2042.9	2045.1	2091.1, 2073.4, 2045.1	ν_s(C−O)[a]
	1998.2	1953.6	1998.2, 1970.4, 1953.6	1952.1	1998.2, 1969.7, 1952.1	ν_{as}(C−O)[b]
	961.6	961.6	961.6	909.4	961.6, 944.3, 909.4	ν_s(W−O)[a]
	901.1	901.1	901.1	856.1	901.1, 870.4, 856.1	ν_{as}(W−O)[b]
	534.6	513.4	534.6, 527.5, 513.4	524.9?	c	ν_{as}(W−C)[b]
O_2WCO	1976.4	1930.6	1976.4, 1930.6	1932.9	1976.4, 1932.9	ν(C−O)
	ca. 903.5	ca. 903.5	ca. 903.5	ca. 857.4	ca. 903.5, 872.3, 857.4	ν_{as}(W−O)[b]
WO	1051.0[d]	1051.0	1051.0	996.1[d]	1051.0, 996.1	ν(W−O)
WCO	1848.8	1807.7	1848.8, 1807.7	1808.4	1848.8, 1808.4	ν(C−O)
$OW(\mu$-CO)$_2$WO	1713.4	1674.5	1713.4, 1691.9, 1674.5	1675.9	1713.4, 1692.8, 1675.9	ν_{as}(C−O)[b]

[a] ν_s refers to the symmetric stretching frequency. [b] ν_{as} refers to the antisymmetric stretching frequency. [c] This feature proved too weak and broad to resolve all the possible isotopomers. For experiments run with $CO_2/C^{18}O_2$, the band though weak appears to be a triplet at ca. 534.6, 531.8, and 528.9 cm^{-1}. [d] The molecule also has two other sites at 1053.8 and 1048.6 cm^{-1} and 998.7 and 993.9 cm^{-1} for WO and W^{18}O, respectively.

For tungsten a similar feature occurs at 534.6 cm^{-1} (*cf.* 526.8 cm^{-1} calculated) in experiments performed with CO_2 as the reactant gas and shifts to 513.4 cm^{-1} (*cf.* 512.5 cm^{-1} calculated) and 528.9 cm^{-1} (*cf.* 524.7 cm^{-1} calculated) in experiments run with $^{13}CO_2$ and $C^{18}O_2$, respectively. Appropriate triplets are weakly observed for reactions with $^{12}CO_2/^{13}CO_2$ and $C^{16}O_2/$

$C^{18}O_2$ as detailed in Table 3; for the experiment with $C^{16}O_2/$ $C^{16}O^{18}O/C^{18}O_2$ the feature proved too broad and weak to resolve the multiplet. In experiments run with CO_2 another feature, which tracks with the rest of the bands due to $O_2W(CO)_2$, proved observable at 409.3 cm^{-1}. This approaches the low-frequency limits of our detection capabilities, and calculations anticipate

Table 4. Calculated Geometries, Frequencies, and Intensities of the OMCO Molecules

(a) OCrCO; $^5A'$ Ground State; C_s Symmetry

Gaussian 94 geometry	$r_{CO} = 1.169$; $r_{CrO} = 1.618$; $r_{CrC} = 1.991$; $\angle OCrC = 123.0°$; $\langle S^2 \rangle = 6.0008$
ADF 2.0.1 geometry	$r_{CO} = 1.157$; $r_{CrO} = 1.622$; $r_{CrC} = 2.000$; $\angle OCrC = 122.1°$

observed frequencies and isotope ratios for O^{52}CrCO			calculated frequencies and isotope ratios using Gaussian 94 (BP86)			calculated frequencies using ADF (LDA + BP)
ν/cm^{-1}	$\nu_{12/13}$	$\nu_{16/18}$	ν/cm^{-1} (I/kmmol^{-1})	$\nu_{12/13}$	$\nu_{16/18}$	ν/cm^{-1} (I/kmmol^{-1})
2014.4	1.022 69	1.023 94	1990.7 (954)	1.023 44	1.023 71	1981.1 (945)
866.3	1.000 00	1.044 36	954.9 (145)	1.000 00	1.045 09	948.8 (171)
			405.0 (6)	1.010 73	1.023 24	400.6 (6)
			304.8 (1)	1.030 77	1.011 62	305.4 (0)
			275.2 (0)	1.029 94	1.012 14	289.1 (0)
			105.8 (12)	1.001 89	1.048 56	112.2 (14)

(b) OMoCO; $^3A'$ Ground State; C_s Symmetry

Gaussian 94 geometry	$r_{CO} = 1.187$; $r_{MoO} = 1.702$; $r_{MoC} = 1.941$; $\angle OMoC = 103.1°$; $\langle S^2 \rangle = 2.0001$
ADF 2.0.1 geometry	$r_{CO} = 1.174$; $r_{MoO} = 1.705$; $r_{MoC} = 1.959$; $\angle OMoC = 109.1°$

observed frequencies and isotope ratios			calculated frequencies and isotope ratios using Gaussian 94 (BP86)			calculated frequencies using ADF (LDA + BP)
ν/cm^{-1}	$\nu_{12/13}$	$\nu_{16/18}$	ν/cm^{-1} (I/kmmol^{-1})	$\nu_{12/13}$	$\nu_{16/18}$	ν/cm^{-1} (I/kmmol^{-1})
1847.0	1.023 67	1.022 65	1902.2 (954)	1.024 23	1.022 58	1900.9 (930)
951.8	0.999 37	1.051 36	964.6 (145)	1.000 00	1.051 91	958.9 (124)
			501.2 (6)	1.011 50	1.028 31	497.5 (5)
			407.3 (14)	1.031 92	1.009 92	399.3 (12)
			372.0 (3)	1.030 47	1.012 24	377.8 (5)
			155.1 (7)	0.999 36	1.054 38	158.0 (8)

(c) OWCO; $^3A'$ Ground State; C_s Symmetry

Gaussian 94 geometry	$r_{CO} = 1.192$; $r_{WO} = 1.699$; $r_{WC} = 1.932$; $\angle OWC = 105.5°$; $\langle S^2 \rangle = 2.0002$
ADF 2.0.1 geometry	$r_{CO} = 1.181$; $r_{WO} = 1.746$; $r_{WC} = 1.958$; $\angle OWC = 104.9°$

observed frequencies and isotope ratios			calculated frequencies and isotope ratios using Gaussian 94 (BP86)			calculated frequencies using ADF (LDA + BP)
ν/cm^{-1}	$\nu_{12/13}$	$\nu_{16/18}$	ν/cm^{-1} (I/kmmol^{-1})	$\nu_{12/13}$	$\nu_{16/18}$	ν/cm^{-1} (I/kmmol^{-1})
1879.0	1.022 86	1.021 86	1882.6 (835)	1.024 54	1.022 04	1868.0 (907)
969.6	1.000 00	1.055 17	990.7 (85)	1.000 00	1.055 62	936.9 (84)
483.8	1.012 98	1.031 34	508.8 (9)	1.011 50	1.028 31	486.6 (6)
			424.6 (2)	1.031 92	1.009 92	403.8 (5)
			398.7 (1)	1.030 47	1.012 24	385.3 (2)
			158.7 (7)	0.999 36	1.054 38	163.2 (9)

that ^{18}O substitution will cause this band to shift out of range (a drop of 12.8 cm^{-1}) whereas ^{13}C substitution results in a shift of 5.9 cm^{-1} which will be difficult to detect. In the absence of isotopic data the assignment of this band to the O$_2$W(CO)$_2$ molecule cannot be definitive, but the band's behavior and relative intensity (approximately the same intensity as the band at 534.6 cm^{-1}) coupled to the results of the theoretical calculations (see Table 5; note that the relative intensities of the low-energy bands are predicted to be the same by Gaussian 94 and of similar magnitude by ADF 2.0.1.) do provide persuasive evidence that this feature is associated with the O$_2$W(CO)$_2$ molecule.

For O$_2$Cr(CO)$_2$ the analogous band occurs at 540.6 cm^{-1} and is shifted to 527.4 and 534.9 cm^{-1} upon isotopic substitution with ^{13}C and ^{18}O, respectively. Isotopic triplets were observed in the reactions with ^{12}CO$_2$/^{13}CO$_2$ and C^{16}O$_2$/C^{18}O$_2$ as detailed in Table 1; for the experiment run with C^{16}O$_2$/C^{16}O^{18}O/C^{18}O$_2$ the feature once again proved too broad and weak to resolve the expected multiplet.

The bands due to the O$_2$M(CO)$_2$ molecules all grow upon annealing to 20 K, are unaffected by broad band UV-photolysis, grow markedly upon annealing to 30 K, and remain at approximately the same intensity at 35 K. The experimentally observed and calculated spectra for all three of these molecules, as detailed in Table 5, prove to be in excellent agreement, and

comparisons between observed and calculated isotope shifts further confirm that the calculations are correctly anticipating the mechanics of vibration of these molecules.

There have been numerous previous studies involving the photolysis of M(CO)$_6$ with O$_2$,[25-28] and bands in these spectra were assigned to the O$_2$M(CO)$_2$ molecules. The CO stretching region in these experiments was extremely congested, but the bands in this region that are observed here for O$_2$Mo(CO)$_2$ and O$_2$W(CO)$_2$ are essentially the same as those observed by Almond *et al.* for their species "C" which was assigned to O$_2$M-(CO)$_x$, not those observed for their species "D" which was assigned to O$_2$M(CO)$_2$.[25] Our results for O$_2$Cr(CO)$_2$ do however confirm the previous correct identification of this molecule.[25,27]

O$_2$MCO. For all three metals there is a prominent feature in the 1800−2100 cm^{-1} region (2037.1, 2000.7, 1976.4) which shifts appropriately upon reaction with ^{13}CO$_2$ (1990.0, 1955.2, 1930.6) and C^{18}O$_2$ (1989.7, 1955.7, 1932.9) to confirm that it is indeed a CO stretch. Reaction with isotopically mixed

(25) Poliakoff, M.; Smith, K. P; Turner, J. J.; Wilkinson, A. J. *J. Chem. Soc., Dalton Trans.* **1982**, 651.
(26) Crayston, J. A.; Almond, M. J.; Downs, A. J.; Poliakoff, M.; Turner, J. J. *Inorg. Chem.* **1984**, *23*, 3051.
(27) Almond, M. J.; Crayston, J. A.; Downs, A. J.; Poliakoff, M.; Turner, J. J. *Inorg. Chem.* **1986**, *25*, 19.
(28) Almond, M. J.; Downs, A. J. *J. Chem. Soc., Dalton Trans.* **1988**, 809.

Table 5. Calculated Geometries, Selected Frequencies, and Intensities of $O_2M(CO)_2$ Molecules

(a) $O_2Cr(CO)_2$; $^1A'$ Ground State; C_s Symmetry

ADF 2.0.1 geometry	$r_{CO} = 1.150$; $r_{CrO} = 1.604$; $r_{CrC} = 1.927$; $\angle OCrC = 106.9°, 107.1°$; $\angle OCrO = 126.0°$; $\angle CCrC = 99.7°$				
observed ν/cm^{-1}	2123.2	2059.7	981.4	941.6	540.6
ADF, ν/cm^{-1} ($I/kmmol^{-1}$)	2065.6 (261)	2012.3 (1003)	1037.9 (187)	1007.3 (16)	569.8 (20)

(b) $O_2Mo(CO)_2$; $^1A'$ Ground State; C_s Symmetry

Gaussian 94 geometry	$r_{CO} = 1.165$; $r_{MoO} = 1.741$; $r_{MoC} = 2.054$; $\angle OMoC = 108.7°$; $\angle OMoO = 124.3°$; $\angle CMoC = 93.4°$; $\langle S^2 \rangle = 0.0000$
ADF 2.0.1 geometry	$r_{CO} = 1.153$; $r_{MoO} = 1.747$; $r_{MoC} = 2.067$; $\angle OMoC = 109.0°$; $\angle OMoO = 123.7°$; $\angle CMoC = 92.9°$

observed frequencies and isotope ratios			calculated frequencies and isotope ratios using Gaussian 94 (BP86)			calculated frequencies using ADF (LDA + BP)
ν/cm^{-1}	$\nu_{12/13}$	$\nu_{16/18}$	ν/cm^{-1} ($I/kmmol^{-1}$)	$\nu_{12/13}$	$\nu_{16/18}$	ν/cm^{-1} ($I/kmmol^{-1}$)
2101.9	1.023 37	1.022 97	2059.7 (283)	1.024 01	1.022 89	2051.9 (311)
2020.1	1.022 63	1.024 03	1997.5 (1009)	1.023 52	1.023 62	1989.9 (1093)
			935.0 (24)	1.000 00	1.055 19	922.7 (25)
885.6	1.000 00	1.046 68	912.4 (180)	1.000 00	1.047 15	898.8 (201)

(c) $O_2W(CO)_2$; $^1A'$ Ground State; C_s Symmetry

Gaussian 94 geometry	$r_{CO} = 1.168$; $r_{WO} = 1.742$; $r_{WC} = 2.042$; $\angle OWC = 109.9°$; $\angle OWO = 121.1°$; $\angle CWC = 92.5°$; $\langle S^2 \rangle = 0.0000$
ADF 2.0.1 geometry	$r_{CO} = 1.155$; $r_{WO} = 1.785$; $r_{WC} = 2.101$; $\angle OWC = 110.9°$; $\angle OWO = 119.0°$; $\angle CWC = 90.8°$

observed frequencies and isotope ratios			calculated frequencies and isotope ratios using Gaussian 94 (BP86)			calculated frequencies using ADF (LDA + BP)
ν/cm^{-1}	$\nu_{12/13}$	$\nu_{16/18}$	ν/cm^{-1} ($I/kmmol^{-1}$)	$\nu_{12/13}$	$\nu_{16/18}$	ν/cm^{-1} ($I/kmmol^{-1}$)
2091.1	1.023 59	1.022 49	2054.1 (276)	1.024 28	1.022 50	2035.2 (311)
1998.2	1.022 83	1.023 62	1989.2 (1046)	1.023 78	1.022 74	1973.6 (1125)
961.6	1.000 00	1.057 40	957.2 (24)	1.000 00	1.057 80	908.8 (28)
901.1	1.000 00	1.052 64	910.8 (154)	1.000 00	1.052 95	857.2 (156)
534.6	1.041 29	1.010 78	528.8 (11)	1.031 80	1.007 51	498.0 (7)
409.3			440.2 (11)	1.013 54	1.029 95	403.1 (11)

samples reveals doublets for this feature, indicative of precisely one CO group. For chromium and molybdenum it proved possible to clearly observe the MO_2 antisymmetric stretching mode (970.5, 876.5), and for chromium the symmetric stretching mode (924.3) also proved sufficiently intense to be observed. The 16/18 isotope ratios for these bands (1.038 97 and 1.046 68 for the antisymmetric stretches of O_2CrCO and O_2MoCO and 1.050 94 for the symmetric stretch of O_2CrCO; cf. 1.045 49 and 1.051 59 calculated harmonic diatomic value) confirm that these motions are due to antisymmetric (lower than the diatomic ratio due to increased metal participation in vibration) and symmetric (higher than the diatomic ratio due to decreased metal participation in vibration) metal oxide stretching modes, respectively. The antisymmetric stretching mode of O_2WCO is partially obscured by the intense band due to $O_2W(CO)_2$. Nevertheless, there is a clear shoulder at higher frequencies on the band due to this molecule (ca. 903.5) which is unaffected by moving from CO_2 to $^{13}CO_2$ but does split into a triplet (ca. 903.5, 872.3, 857.4) upon reaction with $C^{16}O_2/C^{18}O_2$ or $C^{16}O_2/C^{16}O^{18}O/C^{18}O_2$, confirming the presence of two equivalent oxygen atoms. The 16/18 isotopic ratio (1.05377; cf. 1.05553 calculated harmonic WO diatomic) confirms that this is indeed an antisymmetric WO_2 stretching fundamental. For all three molecules the band positions, relative intensities, and isotopic shifts are in excellent agreement with the calculations detailed in Table 6.

MO. The previously characterized metal monoxides MoO (893.5) and WO (1051.0)[29−31] were observed, although in the case of MoO only very weakly. In the experiments run with chromium the metal monoxides CrO (846.5) and $Cr^{18}O$ (809.6) proved to be significant products, and these experiments constituted the first observation of CrO in a matrix (observed at 885.0 cm⁻¹ in the gas phase).[32] All these bands were present

at the same frequencies in reactions with either CO_2 or $^{13}CO_2$, split into doublets upon reaction with $C^{16}O_2/C^{18}O_2$ or $C^{16}O_2/C^{16}O^{18}O/C^{18}O_2$, and shifted appropriately upon reaction with $C^{18}O_2$. Comparison between the observed isotope ratios and calculated harmonic diatomic values confirms the assignment of these bands to the MO molecules. CrO has also now been detected in this laboratory[33] as a product from the reactions of laser-ablated chromium atoms with either O_2 or N_2O. Bands due to CrO_2 were also observed here with CO_2 experiments as well as in the above experiments.[33] Table 7 provides a comparison between the observed and calculated frequencies for the MO and MO_2 molecules.

MCO. The metal monocarbonyls MCO (1975.3, 1862.6, 1848.8) were detected in trace quantities in these experiments. CrCO has been previously characterized,[34] but this represents the first observation of MoCO and WCO, as detailed in Table 7. To confirm these assignments, separate experiments were run in which the metals were ablated into streams of ca. 0.1% CO in Ar, and all of these experiments gave MCO as the dominant product. Reaction with ^{13}CO (1932.4, 1819.2, 1807.7) and $C^{18}O$ (1927.3, 1822.3, 1808.4) confirmed that the absorptions are CO stretches, and experiments run with $CO/^{13}CO$ and $CO/C^{18}O$ revealed appropriate isotopic doublets, confirming the presence of exactly one CO group. Calculations as detailed in Table 7 are in good agreement with the observed data and provide good theoretical support for the assignment of these bands to the metal monocarbonyls. Both WCO and MoCO calculate to be the expected linear, or approximately linear, structure, but CrCO is calculated by ADF to be highly bent.

(29) Devore, T. C.; Gole, J. L. *Chem. Phys.* **1989**, *133*, 95.
(30) Bates, J. K.; Gruen, D. M. *J. Mol. Spectrosc.* **1979**, *78*, 284.
(31) Green, D. W.; Ervin, K. M. *J. Mol. Spectrosc.* **1981**, *89*, 145.

(32) Hocking, W. H.; Merer, A. J.; Milton, D. J.; Jones, W. E.; Krishmanurth, G. *Can. J. Phys.* **1980**, *58*, 516.
(33) Chertihin, G. V.; Bare, W. D.; Andrews, L. *J. Chem. Phys.*, in press.
(34) Bach, S. B. H.; Taylor, C. A.; Van Zee, R. J.; Vala, M. T.; Weltner, W., Jr. *J. Am. Chem. Soc.* **1986**, *108*, 7104.
(35) See for example: Crabtree, R. H. *The Organometallic Chemistry of the Transition Elements*, 2nd ed.; Wiley-Interscience 1994; p 318.

Table 6. Calculated Geometries, Selected Frequencies, and Intensities of the O_2MCO Molecules

(a) O_2CrCO; $^3A''$ (Gaussian 94), $^3A'$ (ADF) Ground State; C_s Symmetry

Gaussian 94 geometry	$r_{CO} = 1.167$; $r_{CrO} = 1.623$; $r_{CrC} = 1.899$; $\angle OCrC = 102.2°$; $\angle OCrO = 108.4°$; $\langle S^2 \rangle = 2.0001$
ADF 2.0.1 geometry	$r_{CO} = 1.144$; $r_{CrO} = 1.668$; $r_{CrC} = 2.050$; $\angle OCrC = 117.5°$; $\angle OCrO = 124.9°$

observed frequencies and isotope ratios			calculated frequencies and isotope ratios using Gaussian 94 (BP86)			calculated frequencies using ADF (LDA + BP)
ν/cm^{-1}	$\nu_{12/13}$	$\nu_{16/18}$	ν/cm^{-1} (I/kmmol^{-1})	$\nu_{12/13}$	$\nu_{16/18}$	ν/cm^{-1} (I/kmmol^{-1})
2037.1	1.023 67	1.023 82	2007.7 (767)	1.023 66	1.023 34	2080.7 (532)
970.5	1.000 00	1.038 97	973.3 (57)	1.000 00	1.043 32	1023.2 (262)
924.3	1.000 00	1.050 94	969.8 (96)	1.000 00	1.044 14	970.1 (36)

(b) O_2MoCO; $^1A'$ Ground State; C_s Symmetry

Gaussian 94 geometry	$r_{CO} = 1.174$; $r_{MoO} = 1.734$; $r_{MoC} = 2.004$; $\angle OMoC = 101.6°$; $\angle OMoO = 118.4°$; $\langle S^2 \rangle = 0.000\ 00$
ADF 2.0.1 geometry	$r_{CO} = 1.161$; $r_{MoO} = 1.740$; $r_{MoC} = 2.021$; $\angle OMoC = 105.7°$; $\angle OMoO = 121.0°$

observed frequencies and isotope ratios			calculated frequencies and isotope ratios using Gaussian 94 (BP86)			calculated frequencies using ADF (LDA + BP)
ν/cm^{-1}	$\nu_{12/13}$	$\nu_{16/18}$	ν/cm^{-1} (I/kmmol^{-1})	$\nu_{12/13}$	$\nu_{16/18}$	ν/cm^{-1} (I/kmmol^{-1})
2000.7	1.023 27	1.023 01	1987.6	1.024 06	1.022 80	1982.5 (754)
			948.8	1.000 00	1.054 81	939.5 (23)
876.5	1.000 00	1.046 94	906.7	1.000 00	1.047 84	899.8 (214)
			473.7	1.011 75	1.027 55	466.6 (3)

(c) O_2WCO; $^1A'$ Ground State; C_s Symmetry

Gaussian 94 geometry	$r_{CO} = 1.178$; $r_{WO} = 1.729$; $r_{WC} = 2.004$; $\angle OWC = 105.5°$; $\angle OWO = 113.0°$; $\langle S^2 \rangle = 0.000\ 00$
ADF 2.0.1 geometry	$r_{CO} = 1.165$; $r_{WO} = 1.769$; $r_{WC} = 2.070$; $\angle OWC = 108.8°$; $\angle OWO = 113.9°$

observed frequencies and isotope ratios			calculated frequencies and isotope ratios using Gaussian 94 (BP86)			calculated frequencies using ADF (LDA + BP)
ν/cm^{-1}	$\nu_{12/13}$	$\nu_{16/18}$	ν/cm^{-1} (I/kmmol^{-1})	$\nu_{12/13}$	$\nu_{16/18}$	ν/cm^{-1} (I/kmmol^{-1})
1976.4	1.023 59	1.022 49	1969.1 (785)	1.024 24	1.022 54	1952.9 (880)
			979.5 (20)	1.000 00	1.057 20	933.7 (23)
903.5	1.000 00	1.053 76	919.5 (133)	1.000 00	1.053 51	873.1 (126)
			470.0 (4)	1.013 59	1.030 48	423.0 (3)

OW(μ-CO)$_2$WO. In the case of the reaction with tungsten, a bridged species, OW(μ-CO)$_2$WO, the dimer of OWCO, is formed. Only the antisymmetric CO stretching mode is observed in a region typical for bridging CO groups. This band observed at 1713.4 cm^{-1} from the reaction of W with CO$_2$ shifts to 1674.5 cm^{-1} on reaction of W with ^{13}CO$_2$ and 1675.9 cm^{-1} on reaction of W with C^{18}O$_2$. It shows a 1:2:1 triplet at 1713.4, 1692.8, and 1675.9 cm^{-1} upon reaction with either C^{16}O$_2$/C^{18}O$_2$ or C^{16}O$_2$/C^{16}O^{18}O/C^{18}O$_2$, and a 1:2:1 triplet at 1713.4, 1691.9, and 1674.5 cm^{-1} upon reaction with a ^{12}CO$_2$/^{13}CO$_2$ mixture, indicating exactly two equivalent CO groups. The product is not observed in similar reactions involving CO, confirming that these absorptions are not due to the molecule W(μ-CO)$_2$W, and its yield is suppressed by using higher concentrations (2%) of CO$_2$, presumably due to further reaction of OWCO with CO$_2$. The lack of a clear candidate for the analogous products for Cr or Mo probably reflects the greater strength of the metal–metal bonding, present in such a complex, of tungsten. DFT calculations using the ADF 2.0.1 program confirm the presence of metal–metal bonding ($r_{W-W} = 2.447$ Å) in this molecule and are presented in Table 7. The agreement between the calculated frequency and the experimentally observed frequency is reasonable for such a molecule.

OCr(CO)$_2$. In the experiments run with chromium the CO stretching region contained a band at 1923.9 cm^{-1} which shifted to 1881.2 and 1878.9 cm^{-1} upon substitution with ^{13}CO$_2$ and C^{18}O$_2$, respectively, confirming this band to be due to a CO stretching motion. Isotopic mixes involving ^{12}CO$_2$/^{13}CO$_2$ revealed a triplet (1923.9, 1897.9, 1881.2), and those with C^{16}O$_2$/C^{18}O$_2$ or C^{16}O$_2$/C^{16}O^{18}O/C^{18}O$_2$ also revealed isotopic triplets (1923.9, 1896.5, 1878.9) indicative of two equivalent CO groups. The CrO stretching mode of this molecule also proved

observable at 891.0 cm^{-1}. Reaction with ^{13}CO$_2$ resulted in little discernible shift, but reaction with C^{18}O$_2$ caused a shift to 853.8 cm^{-1}. This 16/18 isotopic ratio (1.043 57) is indicative of a CrO stretching mode. It is interesting to note the comparison of 16/18 ratios between CrO (1.045 33), OCrCO (1.044 36) and OCr(CO)$_2$ (1.043 57) which reveal a slight decline as more substituents are added as would be expected with increasing antisymmetric O–M–C character from classical mechanical arguments. Reactions with C^{16}O$_2$/C^{18}O$_2$ or C^{16}O$_2$/C^{16}O^{18}O/C^{18}O$_2$ revealed doublets, confirming the presence of exactly one oxygen atom bound to chromium. The feature proved too weak and broad to resolve chromium isotope splittings, but the comparison between the observed frequencies for this molecule and those calculated for OCr(CO)$_2$ using the ADF 2.0.1 code, as detailed in Table 7, confirms the assignment of these bands to the OCr(CO)$_2$ molecule.

Cr(η^1-OCO). CO$_2$ complexes of transition metal atoms are of great interest, not only as models for reactions which take place on metal surfaces but also because studies of their modes of ligation act as guides to the biologically important photosynthesis process whose mechanism is still unclear. The four basic modes of ligation are η^1-**O**CO, η^1-**C**O$_2$, η^2-**O**CO, and η^2-**OC**O, where the atoms coordinated to the metal are indicated in bold. These modes of ligation can be distinguished by their infrared spectra. Bands are observed for this molecule both in the CO stretching region and also in the 750–650 cm^{-1} region. The lower frequency region enables definitive identification of the molecule. Bands at 721.0 and 716.1 cm^{-1} in experiments run with CO$_2$ correspond to two sites of Cr(CO$_2$) complex. These bands shift to 714.1 and 709.0 cm^{-1} upon reaction with ^{13}CO$_2$ and 690.5 and 686.5 cm^{-1} upon reaction with C^{18}O$_2$. Comparison of these isotope ratios ($\nu_{12/13} = 1.0097, 1.0100$;

Table 7. Calculated Geometries, Selected Frequencies, and Intensities of the MO, MO$_2$, MCO, OW(μ-CO)$_2$WO, OCr(CO)$_2$, and Cr(μ-O)(μ-CO)Cr Molecules

(a) MO; $^5\Sigma$ Ground State for CrO; $^3\Sigma$ Ground State for WO; $^3\Sigma$ Ground State for MoO Using Gaussian 94; $^5\Pi$ Ground State for MoO Using ADF 2.0.1

Gaussian 94 geometry	$r_{CrO} = 1.646$, $\langle S^2 \rangle = 6.0002$; $r_{MoO} = 1.717$, $\langle S^2 \rangle = 2.0080$; $r_{WO} = 1.719$, $\langle S^2 \rangle = 2.0175$
ADF 2.0.1 geometry	$r_{CrO} = 1.616$; $r_{MoO} = 1.729$; $r_{WO} = 1.706$

(b) MO$_2$; $^3B_1$ Ground State for M = Cr, Mo; C_{2v} Symmetry; $^1A_1$ Ground State for WO$_2$ Using ADF; $^3B_1$ Ground State for WO$_2$ Using Gaussian 94

Gaussian 94 geometry	$r_{CrO} = 1.607$, $\angle OCrO = 122.8°$, $\langle S^2 \rangle = 2.0011$; $r_{MoO} = 1.723$, $\angle OMoO = 113.5°$, $\langle S^2 \rangle = 2.0000$; $r_{WO} = 1.720$, $\angle OWO = 112.0°$, $\langle S^2 \rangle = 2.0001$
ADF 2.0.1 geometry	$r_{CrO} = 1.609$, $\angle OCrO = 122.2°$; $r_{MoO} = 1.729$, $\angle OMoO = 115.4°$; $r_{WO} = 1.736$, $\angle OWO = 102.9°$

	observed and calculated frequencies for M = Cr ν/cm^{-1} (I/kmmol^{-1})			observed and calculated frequencies for M = Mo ν/cm^{-1} (I/kmmol^{-1})			observed and calculated frequencies for M = W ν/cm^{-1} (I/kmmol^{-1})		
species	obsd	Gaussian	ADF	obsd	Gaussian	ADF	obsd	Gaussian	ADF
MO	846.5	917.9 (137)	941.7 (154)	893.5[a]	954.7 (131)	927.7 (145)	1051.0	966.6[b] (104)	1026.5 (62)
MO$_2$	965.2	1035.9 (244)	1021.3 (275)	948[c]	964.3 (52)	959.4 (48)	975.5[d]	993.3 (40)	1001.7 (32)
	914.4	978.3 (19)	979.3 (21)	899.3[c]	923.6 (188)	916.0 (211)	937.2[d]	932.9 (143)	946.5 (108)
		259.7 (6)	259.5 (3)		299.5 (0)	282.5 (0)		314 (1)	361.6 (2)

(c) MCO; $^7A'$ Ground State for Cr; $^5\Pi$ for Mo; 3A'' for W (Gaussian); $^3\Pi$ for W (ADF)

Gaussian 94 geometry	$r_{CO} = 1.178$, $r_{MoC} = 2.0151$, $\langle S^2 \rangle = 6.0000$; $r_{CO} = 1.189$, $r_{WC} = 1.978$, $\angle OCW = 175.6°$ $\langle S^2 \rangle = 2.0175$
ADF 2.0.1 geometry	$r_{CO} = 1.163$, $r_{CrC} = 2.162$, $\angle OCrO = 137.5°$; $r_{CO} = 1.181$, $r_{MoC} = 1.921$; $r_{CO} = 1.185$, $r_{WC} = 1.924$

	observed frequencies			Gaussian 94 (BP86) ν/cm^{-1} (I/kmmol^{-1})			ADF ν/cm^{-1} (I/kmmol^{-1})
M	MCO	M^{13}CO	MC^{18}O	MCO	M^{13}CO	MC^{18}O	MCO
Cr	1975.3	1932.4	1927.3				1913.9 (930)
Mo	1862.6	1819.2	1822.3	1947.4 (604)	1901.9	1903.6	1871.2 (633)
W	1848.8	1807.7	1808.4	1893.1 (589)	1847.9	1852.1	1852.9 (651)

(d) O$_2$W(μ-CO)$_2$WO; $^1A_{1g}$ Ground State; D_{2h} Symmetry

ADF 2.0.1 geometry	$r_{CO} = 1.185$; $r_{WO} = 1.763$; $r_{WW} = 2.447$			
observed frequencies, ν/cm^{-1}		1713.4		
calculated values, ν/cm^{-1} (I/kmmol^{-1})	1831.9 (0)	1817.2 (1693)	906.0 (0)	905.7 (322)

(e) OCr(CO)$_2$; ^5A Ground State; C_1 Symmetry

ADF 2.0.1 geometry	$r_{CO} = 1.155$; $r_{CrC1} = 2.006$; $r_{CrC2} = 2.007$; $r_{CrO} = 1.6226$; $\angle OCrC_1 = 132.0°$; $\angle OCrC_2 = 132.4°$ $\angle CCrC = 95.7°$	
observed frequencies, ν/cm^{-1}	1923.9	891.0
calculated ADF values, ν/cm^{-1} (I/kmmol^{-1})	1967.7 (1210)	969.2 (198)

(f) Cr(μ-O)(μ-CO)Cr; $^9A_1$ Ground State; C_{2v} Symmetry

ADF 2.0.1 geometry	$r_{CO} = 1.206$; $r_{CrC} = 2.063$; $r_{CrCr} = 2.755$; $r_{CrO} = 1.800$; $\angle OCrC = 88.1°$: $\angle CrCrCr = 83.8°$ $\angle CrOCr = 99.9°$	
observed frequencies, ν/cm^{-1}	1773.8	785.0
calculated ADF values, ν/cm^{-1} (I/kmmol^{-1})	1697.7 (542)	645.8 (47)

[a] In an argon matrix; see ref 30. [b] Run using BPW91 not BP86 owing to convergence problems. [c] In a neon matrix; see: Hewett, W. D., Jr.; Newton, J. H.; Weltner, W., Jr. *J. Phys. Chem.* **1975**, *79*, 2640. [d] In a krypton matrix; see ref 31.

$\nu_{16/18} = 1.044\ 17$, $1.043\ 12$ for the two sites) with the calculated harmonic diatomic CO ($\nu_{12/13} = 1.022\ 80$; $\nu_{16/18} = 1.024\ 76$), CrC ($\nu_{12/13} = 1.032\ 80$), and CrO ($\nu_{16/18} = 1.045\ 51$) ratios reveals this mode to comprise primarily a chromium−oxygen stretch. These isotope ratios rule out the possibility of the η^1-CO$_2$ and η^2-**OCO** modes of coordination as in each case there should be a greater shift on going from ^{12}C to ^{13}C than is observed. Reactions with mixed isotopes revealed a doublet for reactions run with either ^{12}CO$_2$/^{13}CO$_2$ (721.0, 714.1 and 716.1, 709.0 for the two sites) or C^{16}O$_2$/C^{18}O$_2$ (721.0, 690.5 and 716.1, 686.5 for the two sites), but reaction with C^{16}O$_2$/C^{16}O^{18}O/C^{18}O$_2$ revealed a quartet (721.0, 709.3, 703.1, 690.6 and 716.1, 704.1, 698.8, 686.5 for the two sites) indicative of the presence of two *inequivalent* oxygen atoms, both of which must come from the *same* CO$_2$ molecule. This isotopic pattern and 16/18 isotope ratio confirm that the molecule is Cr(η^1-**OCO**) and that the low-frequency bands correspond to a primarily Cr−O stretching mode.

The only other bands observed for this molecule occur in the CO stretching region and are, as expected, more intense than those in the Cr−O stretching region. In principle two bands could be seen due to the symmetric and antisymmetric CO stretches; the symmetric stretch, however, proved too weak to be observed in these experiments. The bands in the CO region for the two sites were broad and overlapped, so the values quoted in Table 1 are only approximate. As can be seen comparison of the observed isotope ratios for the dominant site ($\nu_{12/13} = 1.024\ 07$; $\nu_{16/18} = 1.021\ 60$) and the calculated harmonic diatomic values for CO ($\nu_{12/13} = 1.022\ 80$; $\nu_{16/18} = 1.024\ 76$), reveal this mode to be an antisymmetric CO stretching mode(greater carbon and lesser oxygen motion). Experiments run with ^{12}CO$_2$/^{13}CO$_2$ or C^{16}O$_2$/C^{18}O$_2$ both showed appropriate doublets for the two sites, and experiments run with C^{16}O$_2$/C^{16}O^{18}O/C^{18}O$_2$ showed extra components that were not fully resolvable for the weaker site but were partially resolvable, yielding the anticipated quartet (1735.6, 1732.3, 1702.7, 1698.9) for the dominant site. The yield of this complex was found to increase in experiments in which the chromium target was held a little further from the CsI window. The greater laser spot size results in less ionic species and more metal atoms, with

Table 8. Calculated Energies (kJ mol^{-1}) of Possible Reactions for the M + CO$_2$ Systems, where M = Cr, Mo, orW, Using Both the ADF 2.0.1 and Gaussian 94 Codes

	reaction	ΔE (ADF)			ΔE (Gaussian)		
		Cr	Mo	W	Cr	Mo	W
(1)	M + CO$_2$ → OMCO	−14.1	−301.6	−228.3	+6.5	−286.3	−347.6
(2)	M + 2CO$_2$ → O$_2$M(CO)$_2$	−186.9	−548.2	−431.3		−505.1	−665.7
(3)	OMCO → MO + CO	+208.4	+188.0	+105.9	+212.6	+282.2	
(4)	O$_2$M(CO)$_2$ → O$_2$MCO + CO	+162.3	+197.6	+173.5		+198.0	+380.4
(5)	OMCO + CO$_2$ → O$_2$MCO + CO	−10.5	−49.0	−29.7	99.9	−26.9	−81.8
(6)	M + CO$_2$ → MO + CO	+194.0	−113.6	−122.2	+219.1	−4.1	
(7)	OMCO + CO$_2$ → O$_2$M(CO)$_2$	−172.9	−246.6	−203.2		−218.8	−318.1
(8)	O$_2$MCO → MO$_2$ + CO	+130.7	+150.6	+88.7	+48.6	+166.2	+184.2
(9)	O$_2$Cr(CO)$_2$ → OCr(CO)$_2$ + O	+693.6					
(10)	Cr + O$_2$Cr(CO)$_2$ → OCr(CO)$_2$ + CrO	+263.5					
(11)	2OWCO → OW(μ-CO)$_2$WO			−155.8			
(12)	OCrCO + Cr → Cr(μ-O)(μ-CO)Cr	−188.6					

less excess electronic energy being present in the gas phase. These effects coupled to the decreased brightness of the laser plume have hence been shown to favor complex formation over direct insertion of Cr into CO$_2$.

These findings are in excellent agreement with a previous theoretical study on the interaction between Cr and CO$_2$[11] which showed the lowest energy complex (and indeed the only complex to be stable with respect to disproportionation to Cr and CO$_2$) to be the Cr(η^1-**O**CO) molecule with a Cr−O bond length of 1.92 Å. Attempts to calculate this complex resulted in convergence problems.

Perhaps of greatest interest is the dramatic photochemistry that this molecule displays. Broad band UV-photolysis with a 175 W lamp for 20−30 min results in almost complete destruction of the complex with a concomitant growth in the features due to the insertion product OCrCO. This is, we believe, the first observation of a well-characterized photoinduced insertion of a transition metal atom into carbon dioxide. The use of photolysis to activate CO$_2$ is of enormous potential significance in the development of CO$_2$ as an alternative to petroleum as a starting material for fine chemical synthesis. Studies of the preferred mode of ligation of CO$_2$ to metal centers may also lend further credence to the hypothesis that the CO$_2$ used in photosynthesis is polarized due to formation of an η^1-**O**CO complex to the active enzyme ribulose diphosphate carboxylase prior to attack by the enolate anion of the sugar.[34]

Other Bands. In the Cr/CO$_2$ experiments additional bands were observed in both the bridging CO and Cr−O single bond regions. Upon higher temperature annealings, these two bands, which exhibited the same relative intensities under all conditions, were observed to grow at 1773.8 and 785.0 cm^{-1} in the reactions of Cr with CO$_2$, but were not present in reactions run with Cr and CO. These bands shifted to 1736.8 and 783.4 cm^{-1} upon reaction with ^{13}CO$_2$ and 1737.2 and 746.7 cm^{-1} upon reaction with C^{18}O$_2$. The mode at higher frequency exhibits isotope ratios($\nu_{12/13}$ = 1.021 30; $\nu_{16/18}$ = 1.021 06) indicative of a CO stretching mode. The lower frequency band has a much higher than diatomic 16/18 isotopic ratio($\nu_{16/18}$ = 1.051 29; *cf.* 1.045 49 calculated diatomic harmonic value). Reaction with CO$_2$/^{13}-CO$_2$ mixtures result in appropriate isotopic doublets (1773.8, 1736.8 and 785.0, 783.4) as do reactions with either C^{16}O$_2$/C^{18}O$_2$ or C^{16}O$_2$/C^{16}O^{18}O/C^{18}O$_2$ (1773.8, 1737.2 and 785.0, 746.7). The high 16/18 isotopic ratio for the lower frequency band is indicative either of a MO$_2$ symmetric stretch, which can be conclusively ruled out as this band would become a triplet in reactions run with C^{16}O$_2$/C^{18}O$_2$ and have an associated antisymmetric mode of greater intensity, or of an antisymmetric CrOCr stretch. The latter is totally consistent with the band positions, isotope shifts, and isotopic patterns displayed. The

spectroscopic observations strongly imply that the molecule responsible for these absorptions is Cr(μ-O)(μ-CO)Cr. The molecule is almost certainly formed by reaction of Cr with OCrCO as the bands due to OCrCO are observed to diminish upon higher annealings as the bands due to this molecule grow. The small shift in the frequency of the lower frequency band upon substitution with ^{13}C provides further confirmation of the validity of the assignment as the CrOCr stretch is expected to couple with the CrCCr stretch in such a molecule, resulting in a shift on the order of that observed. Attempts to calculate this molecule using Gaussian met with convergence problems, but the results of the ADF calculations are presented in Table 7. The agreement between theory and experiment is only moderate, with calculations seemingly overplaying the donation of electron density into the CO Π* orbitals at the expense of the Cr−O bonding. The calculations reveal no Cr−Cr bonding (r_{CrCr} = 2.755) in this complex.

Reaction Mechanisms and Periodic Trends

A summary of the calculated energetics of reaction for some of the possible reactions between Cr, Mo, and W and CO$_2$ is presented in Table 8. As can be seen insertion of the metal into CO$_2$ is an exothermic process for Mo and W (eq 1), as indeed is further reaction with another CO$_2$ molecule (eq 2 and 7) for all three metals. Reaction of Cr with CO$_2$ is calculated to be either slightly exothermic or slightly endothermic depending on the theoretical method chosen. Several effects are apparent upon comparing the energetics of the various product molecules from the reactions of Cr, Mo, and W with CO$_2$. Firstly the increased strength of the M−O bond on descending the group is reflected in the calculated energies. This lower bond strength for chromium-containing species coupled to the loss of exchange energy and large pairing energy terms that such products suffer contribute toward a general increased endothermicity of reactions involving gaseous Cr. For example, the reaction of M with CO$_2$ to give MO and CO (eq 6) is calculated by ADF to be exothermic for both W and Mo, but endothermic for Cr. That molecules such as CrO are observed attests to the excess energy that laser-ablated metal atoms possess.[36]

Both theoretical methods chosen were in close agreement with the observed values and the isotope ratios calculated using the Gaussian 94 code, and those observed experimentally confirmed that these calculations are able to accurately predict the mechanics of vibration for such molecules. Generally few problems were encountered for the calculations involving Mo and W using either code, and the results obtained by the two methods are strikingly similar (see Tables 4−7). Calculations

(36) Kang, H.; Beauchamp, J. L. *J. Phys. Chem.* **1985**, *89*, 3364.

involving chromium proved more problematical, especially when the Gaussian 94 code was used, where severe convergence problems were often encountered. Even when the calculations did not prove very accurate their predicted trends were generally still correct. For instance, both ADF 2.0.1 and Gaussian 94 consistently overestimated the Cr−O stretching frequencies, but the observed trend of increased frequency from CrO_2 to O_2-CrCO to $O_2Cr(CO)_2$ was indeed correctly anticipated by ADF. Generally the calculations using Gaussian 94 proved more convenient as the program allows facile determination of the effects of isotopic substitution, but for calculations involving chromium or larger molecules such as $OW(\mu\text{-}CO)_2WO$, as well as the diatomic WO, where the calculations within Gaussian 94 encountered severe convergence problems, ADF 2.0.1 proved the method of choice.

Comparing the molecules MO and OMCO, it can be seen that the W−O stretching frequency is greater than the Mo−O stretching frequency which is in turn greater than the Cr−O stretching frequency for both molecules. Relativistic effects for tungsten are anticipated to be of importance[37] and should result in a greater spatial extension, and hence better overlap, of the 5d orbitals of tungsten relative to the 4d orbitals of molybdenum and can thus be used to explain why the WO stretching frequencies are higher than the MoO stretching frequencies for all these molecules. The synergic nature of the bonding with CO coupled to the different ground state multiplicities of the MCO, MO, and OMCO as well as the MO_2, O_2MCO, and

$O_2M(CO)_2$ series precludes sweeping generalizations about their behaviors upon changing the metal M. Nevertheless, chromium is much less able to back-bond with CO than the other two metals (reflected in a greater ν_{CO} for all complexes with M = Cr) due in part to the contracted nature, and hence poor overlap, of its 3d orbitals and its preference for high spin states owing to a relatively large pairing energy term. The tungsten compounds generally showed the greatest extent of back-bonding with CO, with one notable exception, OMCO, for which molybdenum had the lower CO stretching frequency.

Conclusion

Reaction of laser-ablated group 6 atoms with CO_2 gives rise to a variety of products, including the insertion products OMCO and $O_2M(CO)_2$. Chromium reacts with CO_2 to form a Cr (η^1-**O**CO) complex which undergoes photoinduced isomerization to give OCrCO. Isotopic substitution has allowed definitive spectral identification of these molecules. Theoretical calculations have been used to lend support to these assignments; two DFT-based methods were employed, one using the Gaussian 94 code and the other ADF 2.0.1. Both methods gave results in excellent agreement with the spectroscopic observations, further confirming their validity in the prediction of the frequencies of compounds containing transition metals.

(37) Pyykkö, P. *Chem. Rev.* **1988**, *88*, 563.